



Ricky Wai Kiu Cheung
Graduate Engineer, Mott
Macdonald, Hong Kong



Songdong Shao
Lecturer in Environmental
Fluid Mechanics, University of
Bradford, Bradford, UK

Revisiting a flood simulation model based on PIC techniques

R. W. K. Cheung MEng and S. Shao MSc, PhD, FHEA

A simple and effective two-dimensional flood simulation model based on particle-in-cell (PIC) techniques is revisited. The model solves shallow water equations using a combination of fixed grids and moving particles. In the computation, each fluid particle follows the law of motion induced by gravitational, frictional and viscous forces. The velocity and position of the particles are relocated at each individual grid point in the computational domain to give a macro-flow scenario. By using a documented flood case that happened in the Jingjiang River flood diversion area in China in 1954, the sensitivity of several model parameters is investigated. The convergence and accuracy of the model are demonstrated by adjusting the time steps and particle numbers. The spatial resolution of the proposed method is quantified using numerical error analysis. The predicted flood level is in general agreement with the observed data.

NOTATION

A	area of square grid region
$a_{b,t}$	acceleration of particle b at time t
C	wave celerity
CR	order of convergence
$E_{\Delta V}$	numerical error with accurate solution
g	gravitational acceleration
H	water surface elevation
h	flow depth
$h_{b,t}$	flow depth at location of particle b
h_{ij}	flow depth at grid point
h^s	sample values of flow depth for error analysis
N_{ij}	number of particles near grid point
n	roughness of bed
$n_{b,t}$	roughness of bed at location of particle b
Q	flow discharge at flow inlet
$S_{b,t}$	water surface slope at location of particle b
v	flow velocity
v_{ij}	flow velocity at grid point
v_b	velocity of particle b
$X_{b,t}$	spatial coordinates of particle b at time t
α	Courant coefficient
ΔS	constant grid spacing in x and y directions
Δt	time increment
ΔV	volume of fluid particle
μ	dynamic viscosity
ρ	density of water

1. INTRODUCTION

Climate change and man-made damage to the natural environment are resulting in increased levels of destructive flooding causing loss of property and human life. For example, within the UK there are currently over a million properties at risk and sea levels are about 10 cm higher than they were a few hundred years ago. Prediction of flooding processes is therefore of significant theoretical interest and practical importance. Although field investigations and laboratory experiments have provided invaluable information in this regard, an appropriately established and calibrated numerical model could provide a timely and economic evaluation of flood route, arrival time, water level variations, etc.

Many researchers have developed numerical models to differing levels to predict flooding processes. For example, Caleffi *et al.* (2003) developed a two-dimensional (2D) computer code based on shallow water equations (SWEs) using the Godunov finite-volume method to simulate an extreme flood event in an Italian river valley. Werner and Lambert (2007) used several computer codes to compute the flood discharges in different geometries of compound channels and compared their results with the predictions of empirical and theoretical models. More sophisticated 3D flood simulations using the Navier–Stokes equations have also been carried out to study the complicated flow structures in a natural river floodplain (Nicholas and Mclelland, 2004). Most studies have indicated that one of the most efficient ways to simulate flooding on a large horizontal scale is to use the SWEs and model the river bottom resistance through a semi-empirical approach. The SWE model can be solved by a variety of numerical solvers; the finite-volume approach based on the MUSCL reconstruction with an approximate Riemann solver (Mingham and Causon, 1998) is widely used.

For practical purposes, especially in the initial flood evaluation stage, a simple and effective simulation tool that can be easily understood by engineers would be most useful. The particle-in-cell (PIC) method originally developed by Harlow (1964) has been shown to be a robust approach as there are no complicated algorithms involved and the model output is quite satisfactory. Tetzlaff and Harbaugh (1989) applied this model to geological sedimentation and a new generation of commercial software (e.g. Sedsim) has come into being as a result. Sedsim is a software program that determines how sediments change in both time and space by recreating the

physical processes that deposit, erode and rework sediments; it is extremely useful in the oil industry. Wang *et al.* (1998) used the original PIC approach (Harlow, 1964) to reproduce a documented flood event near the Jingjiang River within the Yangtze River catchment and Shao *et al.* (2002) modified the PIC approach combined with a non-Newtonian rheological model to simulate mud flow deposition in the Jiangjia Valley in Yunnan, China.

In this paper the original PIC method is revisited to investigate its numerical convergence and accuracy by using a set of numerical tests. Unlike the work of Wang *et al.* (1998) in which water level agreement was found, the present study focuses more on the numerical scheme analysis. Temporal and spatial resolutions are quantified by alternating time steps and particle numbers in the computational domain. A sensitivity analysis of the influence of bed roughness on flooding is made in order to provide information with which to reduce the peak flood level and change the flood arrival time. Moreover, the viscous term, which was omitted by Wang *et al.* (1998), is included in the SWEs to address the interactions between different portions of the fluid with different flow velocities.

2. HORIZONTAL 2D PIC MODEL

2.1. Governing equations

The following SWEs are used in the model, which includes the continuity and momentum equations

$$1 \quad \frac{\partial h}{\partial t} + \nabla(hv) = 0$$

$$2 \quad \frac{dv}{dt} = \frac{\partial v}{\partial t} + (v\nabla)v \\ = -g\nabla H - gn^2 \frac{v|v|}{h^{4/3}} + \frac{\mu}{\rho} \nabla^2 v$$

where h is flow depth, t is time, v is flow velocity, g is gravitational acceleration, H is water surface elevation, n is the bed roughness, μ is dynamic viscosity and ρ is the density of water. The left-hand side of Equation 2 is written in Lagrangian form to be used for each individual particle. The three terms on the right-hand side of Equation 2 correspond, respectively, to the accelerations induced by the gravitational force, the bed friction force modified from the Manning's formula and the viscous force arising from the different velocities of the surrounding fluids.

2.2. Principles of the PIC model

The PIC model is a combined Lagrangian–Eulerian approach based on the assumptions that the entire water medium is an assembly of many small, identical and homogeneous water particles (Harlow, 1964). In a horizontal 2D flow, flow occurs only in the two horizontal dimensions, thus the motion of each particle follows the previous SWEs. The SWEs are solved through a step-by-step numerical integration in the time domain. Consequently, the velocity and spatial positions of all the particles are obtained. By averaging these parameters at the prescribed grid points in the computational area, the overall flow behaviour can be understood.

Flow parameters including topographic elevation, flow depth and velocity are represented at the fixed points on a 2D square grid covering the modelled area, while other flow parameters such as the velocity and spatial positions of each water particle are represented for the particle that moves with the flow.

Flow parameters at the grid point represent the averages within a square region surrounding each grid point. For example, the flow depth at a grid point is calculated by

$$3 \quad h_{ij} = \frac{N_{ij}\Delta V}{A}$$

where h_{ij} is the flow depth at grid point ij , N_{ij} is the number of water particles within the square area surrounding the grid point, ΔV is the volume of one particle and A is the area of the square grid region. Equation 3 was actually derived from the continuity equation given in Equation 1 and thus the mass conservation of the PIC model can be simply satisfied without additional numerical procedures.

Similarly, the flow velocity at a grid point is calculated as the average velocity of all particles within the square grid region surrounding the grid point

$$4 \quad v_{ij} = \frac{1}{N_{ij}} \sum_{b=1}^{N_{ij}} v_b$$

where v_{ij} is the flow velocity at grid point ij and v_b is the velocity of water particle b .

Applying the first-order finite-difference principle in time and second-order finite-difference principle in space to Equation 2, the motion of each water particle is computed from (Tetzlaff and Harbaugh, 1989)

$$5 \quad \frac{v_{b,t+\Delta t} - v_{b,t}}{\Delta t} = gS_{b,t} - gn_{b,t}^2 \frac{v_{b,t}|v_{b,t}|}{h_{b,t}^{4/3}} \\ + \frac{\mu}{\rho} \frac{(v_{i,j+1}^t + v_{i,j-1}^t + v_{i+1,j}^t + v_{i-1,j}^t) - 4v_{ij}^t}{(\Delta S)^2}$$

where $v_{b,t+\Delta t}$ and $v_{b,t}$ are the velocity of particle b at time $t + \Delta t$ and t , respectively; Δt is the time increment; $S_{b,t}$ is the water surface slope at the location of particle b ; $n_{b,t}$ is the bed roughness at the location of particle b ; $h_{b,t}$ is flow depth at the location of particle b ; v_{ij}^t is flow velocity at grid point ij at time t ; and ΔS is the grid spacing in both x and y directions if a constant grid is used. The ij in v_{ij}^t corresponds to the grid point that is closest to particle b . The evaluation of water surface slope $S_{b,t}$ requires interpolation between the values at neighbouring grid points and a bi-quadratic interpolation function as proposed by Tetzlaff and Harbaugh (1989) is followed.

The last term on the right-hand side of Equation 5 represents the viscous friction force arising from different layers of the fluid with different flow velocities. Thus it is very useful to maintain a smoother flow field and eliminate unrealistic particle fluctuations. This viscous term is represented in a

standard second-order finite-difference form based on an Eulerian grid to have a clear physical interpretation and concise coding. An open-channel flume experiment carried out by Tetzlaff and Harbaugh (1989) showed typical values of μ to be around 100 Pa s, but it can vary according to different flow conditions.

If the summation on the right-hand side of Equation 5 is $\mathbf{a}_{b,t}$, the updated velocity of water particle b is

6	$\mathbf{v}_{b,t+\Delta t} = \mathbf{v}_{b,t} + \mathbf{a}_{b,t}\Delta t$
---	---

The spatial position of the particle is then computed from

7	$\mathbf{X}_{b,t+\Delta t} = \mathbf{X}_{b,t} + \frac{\mathbf{v}_{b,t+\Delta t} + \mathbf{v}_{b,t}}{2} \Delta t$
---	--

where $\mathbf{X}_{b,t+\Delta t}$ and $\mathbf{X}_{b,t}$ are the spatial coordinates of particle b at time $t + \Delta t$ and t , respectively.

2.3. Initial and boundary conditions

The prescription of initial and boundary conditions in the proposed PIC model is straightforward. Initial conditions just need to provide the topographic elevation at all the grid points at the beginning of computation. If the modelled domain initially contains the flow, then the velocity and spatial coordinates of existing water particles also need to be specified. The flow depth and velocity at grid points can be then computed from Equations 3 and 4.

Two kinds of boundary conditions are required. The inflow boundary conditions provide the input of water particles according to the inflow discharge hydrograph. The number and velocity of these input particles can be evaluated according to the available discharge Q at the flow inlet, the volume of each particle ΔV and time increment Δt in the computations. Wall boundary conditions are provided at the side walls or river banks that are incorporated into the computational domain. The velocity at these grid points is set zero to represent the non-slip boundary. In the computations, the water particles change direction after colliding with these physical boundaries. They also lose a fraction of energy and momentum during the impact. As there is no theoretical method available to evaluate the impact process, for simplicity the collision process is assumed to be elastic, except that the velocity of particles after the collision is reduced by half to approximate the energy loss (Shao *et al.*, 2002; Wang *et al.*, 1998).

3. MODEL APPLICATION AND RESULTS ANALYSIS

3.1. Background information

The Jingjiang River, located in the middle and lower reach of the Yangtze River in China, is subject to frequent flooding in summer. To protect the downstream industrial cities, a flood diversion area was built near the Jingjiang River to store flood water. The Jingjiang River flood diversion region covers an area of 960 km² and the surrounding land boundaries extend to a length of 200 km. The maximum length of the diversion region is 70 km from north to south and the maximum width is 30 km from west to east. The total drop in topographic elevation is 10 m, with an average longitudinal slope of 1.5/

10 000. A plan view of the flood diversion region is shown in Figure 1. Three gauging stations, at Ma Jiazui, Huang Jinkou and Huang Tianhu, were set up when the flood diversion was put into operation in 1954 to monitor flood arrival and water level variations. For the real 1954 flood event, the inlet flow lasted 300 h and the total discharge volume was 4.0×10^9 m³. The inlet discharge hydrograph given in Table 1 defines the inflow boundary conditions.

The computational area is divided into 960 square cells with a grid spacing $\Delta S = 1000$ m in both horizontal and vertical directions. This grid size was selected as the original topographic elevations were measured at an interval of 1000 m. In the model sensitivity test, the main purpose is to evaluate the convergence of the method related to particle number. Thus there is no additional analysis carried out on the grid spacing. The selection of bed roughness n is one of the key parameters used to simulate the flood process realistically. The following values, based on the local flood bureau report (Li and Huang, 1993), were used depending on bed conditions

- (a) $n = 0.025$ for low-resistance regions such as ground surfaces and small rivers
- (b) $n = 0.05$ for moderate-resistance regions such as trees and crops
- (c) $n = 0.1$ for high-resistance regions such as farmhouses and other buildings.

3.2. Sensitivity test on time step Δt

Equations 3 and 4 indicate that a water particle is allocated to its nearest grid point for the calculation of relevant flow parameters. The rapid and large translation of many particles during one time step Δt can lead to instabilities in the numerical computation. The value of Δt should thus be restricted to ensure that the maximum translation distance of

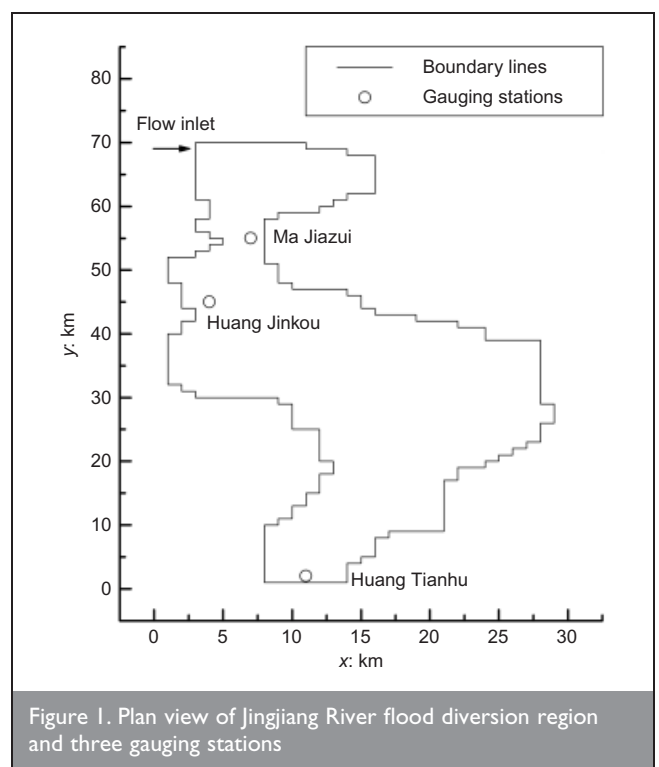


Figure 1. Plan view of Jingjiang River flood diversion region and three gauging stations

Time: h	Discharge: m ³ /s
0	0
24	6400
48	5900
72	5600
96	4200
144	0
171	0
180	5600
192	6600
216	6700
240	5500
254	0
258	0
264	2600
288	5100
300	3700

Table 1. Inflow discharge hydrograph at Jingjiang River flood diversion region in 1954

each particle within a time step is less than a fraction of the grid spacing

$$8 \quad |X_{b,t+\Delta t} - X_{b,t}| < \alpha \Delta S$$

This constraint is used to control Δt in the computation and is equivalent to the Courant condition in explicit time stepping. From the formulation of the PIC model in the previous section, we can see that the numerical scheme is fully explicit based on the finite differencing and thus the Courant condition should be applied.

The value of the Courant coefficient α will be determined in the following numerical tests. Three different time steps (10, 20 and 30 s) were used to test the stability of the model. The volume of water particles was fixed as $\Delta V = 100 \times 10^3 \text{ m}^3$ in all the runs. This paper presents results at Ma Jiazui and Huang Tianhu gauging stations. The total simulation time was over 400 h.

As may be seen in Figure 2, there is not much difference in the computations using $\Delta t = 10$ and 20 s, but the computations using $\Delta t = 30$ s look obviously unrealistic, with this time step underestimating flow depth by nearly 50%. Figure 2 indicates an average water depth of around 3.0–4.0 m. It is reasonable to use the gravity wave celerity $C = (gh)^{1/2}$ to yield a wave speed of 6.0 m/s to approximate the maximum water particle velocity in the computation. The maximum time step $\Delta t = 20$ s in a stable computation leads to a maximum particle displacement of 120 m within Δt . As the grid spacing was selected as $\Delta S = 1000$ m, it can be concluded that the stability coefficient (i.e. the Courant coefficient α in Equation 8) should be around 0.12 in this test.

This calculated Courant coefficient is quite small; for an explicit method, it can reach 0.8. It was found that this issue is related to the choice of particle volume. As the employed particle size is relatively large, it could impose a stricter requirement on numerical stability. To numerically prove this, another run was carried out with a smaller particle volume of

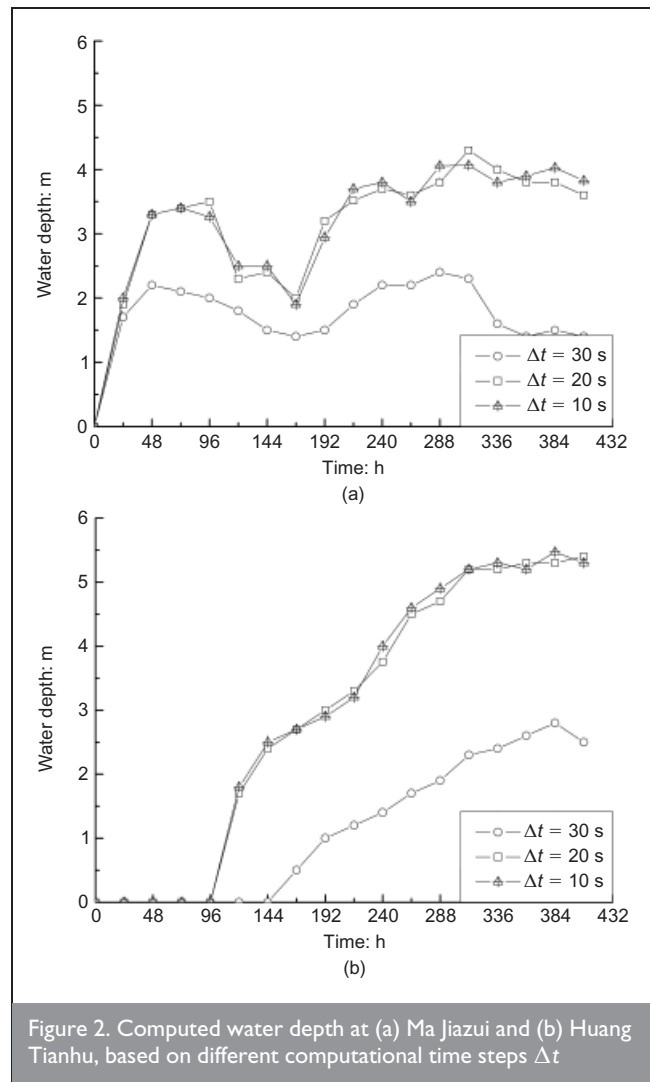


Figure 2. Computed water depth at (a) Ma Jiazui and (b) Huang Tianhu, based on different computational time steps Δt

$\Delta V = 50 \times 10^3 \text{ m}^3$; this yielded a Courant coefficient of 0.25. Although a larger time step was used, the computation time actually increased due to the doubling of the numbers of fluid particles and thus more loops being executed in the numerical program.

3.3. Sensitivity test on particle volume ΔV and error analysis

Because the individual water particles are discrete points and cannot deform as a real flow does, the number of particles employed in the computation must be sufficiently large to give a realistic flow simulation. This requirement is essential for numerical convergence. Thus convergence can be achieved by increasing the number of particles (or equivalently decreasing the volume of each particle) into the computational domain until the numerical solutions are essentially unchanged.

To quantify the convergence process, three different particle sizes ($\Delta V = 200 \times 10^3$, 100×10^3 and $50 \times 10^3 \text{ m}^3$) were used and the computed water depths are shown in Figure 3. To eliminate the influence of the time step, Δt was fixed for all three runs. Figure 3 clearly shows that as particle numbers increase (or particle volumes decrease) the computed water depth curves converge. These tests qualitatively indicate convergence of the model with an increase in particle numbers.

To quantify the accuracy of the proposed PIC numerical

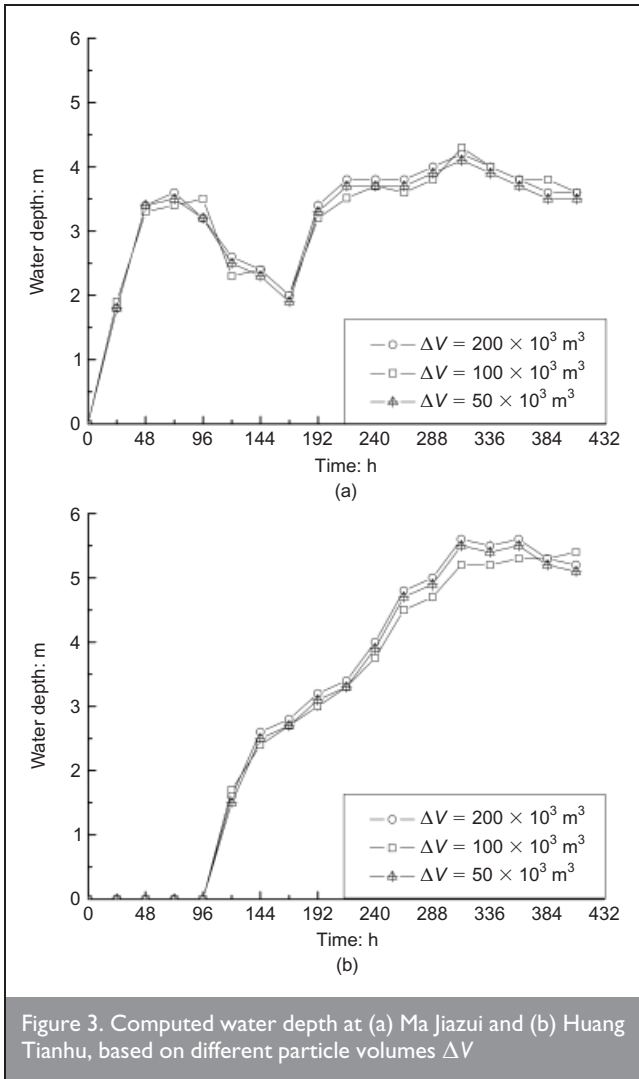


Figure 3. Computed water depth at (a) Ma Jiazui and (b) Huang Tianhu, based on different particle volumes ΔV

scheme with particle volume ΔV , the three numerical trials in Figure 3 can be used for numerical error analysis. A similar approach was employed by Ogami (1999) to analyse a Lagrangian scheme for a compressible flow. According to Ogami's study, the numerical error $E_{\Delta V}$ of any run with an accurate solution is proportional to a function of the particle volume $(\Delta V)^{CR}$, where CR is the order of convergence. If we let $E_{200 \times 10^3}$, $E_{100 \times 10^3}$ and $E_{50 \times 10^3}$ be the numerical differences between adjacent runs using particle volumes of 200×10^3 , 100×10^3 and 50×10^3 m³, then the following relationship can be established to relate numerical error with particle volume

$$9 \quad \frac{E_{200 \times 10^3} - E_{100 \times 10^3}}{E_{100 \times 10^3} - E_{50 \times 10^3}} = \frac{E_{200 \times 10^3, 100 \times 10^3}}{E_{100 \times 10^3, 50 \times 10^3}} \approx \frac{(\Delta V_{200 \times 10^3})^{CR} - (\Delta V_{100 \times 10^3})^{CR}}{(\Delta V_{100 \times 10^3})^{CR} - (\Delta V_{50 \times 10^3})^{CR}}$$

According to the design of numerical trials

$$10 \quad \Delta V_{200 \times 10^3} = 2\Delta V_{100 \times 10^3} = 4\Delta V_{50 \times 10^3}$$

Thus Equation 9 simplifies to

$$11 \quad \frac{E_{200 \times 10^3, 100 \times 10^3}}{E_{100 \times 10^3, 50 \times 10^3}} \approx 2^{CR}$$

To calculate the numerical differences between two adjacent runs, the following sampling method was applied to Figure 3

$$12 \quad E_{200 \times 10^3} - E_{100 \times 10^3} = h_{200 \times 10^3}^s - h_{100 \times 10^3}^s$$

$$13 \quad E_{100 \times 10^3} - E_{50 \times 10^3} = h_{100 \times 10^3}^s - h_{50 \times 10^3}^s$$

where $h_{200 \times 10^3}^s$, $h_{100 \times 10^3}^s$ and $h_{50 \times 10^3}^s$ are sample values of the flow depth and the sample points s are uniformly distributed along the horizontal time axis as shown in Figure 3. Each sample point corresponds to a specified CR. If enough points are used to obtain a series of CR, the mean value can then be used to represent the order of convergence.

Using 100 points from Figure 3, the mean value of CR was calculated to be around 1.2. Thus the accuracy of the proposed PIC numerical scheme with regard to particle volume ΔV can be represented by $O(\Delta V^{-1.2})$, which indicates that it is first-order-accurate globally. This conclusion is also consistent with the PIC model formulations from Equations 3–7 and the interpolation scheme of water surfaces, which are most essentially based on the first-order-accurate scheme. However, the inclusion of the central second-order-accurate finite-difference scheme in Equation 5 for the viscosity term increased the spatial accuracy of the model, leading to the final numerical scheme being slightly higher than first order.

3.4. Model verifications

To validate the accuracy of the computations, the computed water depths in Figure 3 are compared with measured data (Li and Huang, 1993) in Figure 4. The general agreement is quite satisfactory.

At the first gauging station at Ma Jiazui (Figure 4(a)), the documented first flood peak arrives at 75 h and the corresponding water depth is 3.4 m; the numerical model predicted an arrival time of 70 h and a water depth of 3.5 m. The documented data indicate the first flood trough at 170 h with a corresponding minimum water depth of 2.1 m, while the numerical model predicted an arrival time of 165 h and a water depth of 1.9 m. At Huang Tianhu (Figure 4(b)), the measured data showed a flood arrival time of 80 h and a continuous water depth increase up to 5.0 m at time $t = 300$ h. In contrast, the numerical model predicted a flood arrival time of 92 h and water depth of 5.2 m at time $t = 300$ h. It seems that even the roughest computations using $\Delta V = 200 \times 10^3$ m³ can still give a realistic prediction of general flood features. Compared with the results of Wang *et al.* (1998), the present computations use a relatively coarse spatial resolution and the computation time has been considerably reduced.

3.5. Influence of bed roughness n

To study the influence of bed roughness n on the flood arrival time and peak flood levels, three tests were carried out using bed roughnesses of $n = 0.025$, 0.05 and 0.10 corresponding to different resistance conditions in the flood diversion area. The

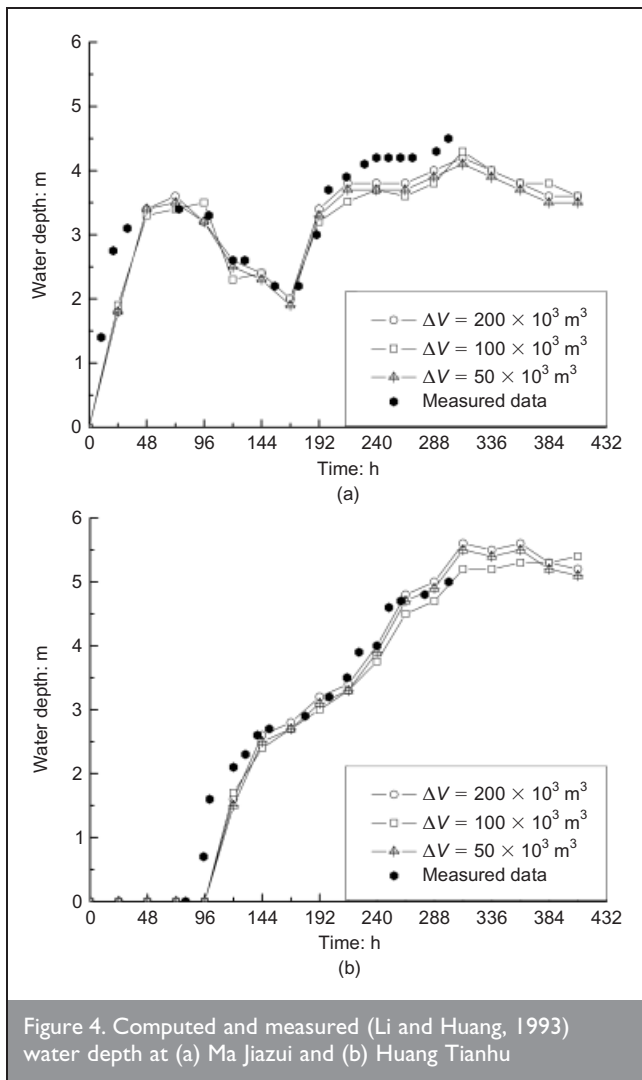


Figure 4. Computed and measured (Li and Huang, 1993) water depth at (a) Ma Jiazui and (b) Huang Tianhu

computed water depths at Ma Jiazui and Huang Tianhu are shown in Figure 5.

As shown in Figure 5(a), computations with a larger value of n give a delayed peak flood arrival time and a much higher flood level at the upstream gauging station of Ma Jiazui, in which the peak flood level computed using $n = 0.1$ at time $t = 84$ h is about 1.4 m higher than that computed using $n = 0.025$ at time $t = 48$ h. The computed flood trough at 168 h is also 1.2 m higher. Similarly, for the downstream gauging station at Huang Tianhu, the flood arrival time was delayed by 48 h for the computation using $n = 0.1$ as compared with that using $n = 0.025$. However, the flood levels computed using $n = 0.1$ are generally 0.5–2.5 m lower, which is quite different from the upstream situation. This phenomenon can be explained as follows. As shown from the numerical model, the energy loss of water particles is proportional to bed roughness in the flood diversion area and the movement of particles will reduce when bed roughness increases. As a result, the flood levels in the upstream area increase considerably due to the accumulation of local water particles. The flood arrival time in both upstream and downstream areas can also be delayed due to the slow motion of water. Unlike in the upstream region, the flood levels in the downstream area actually decrease when bed roughness increases as more flood water is retained upstream. However, as shown in Figure 5, in the later stage of flood diversion

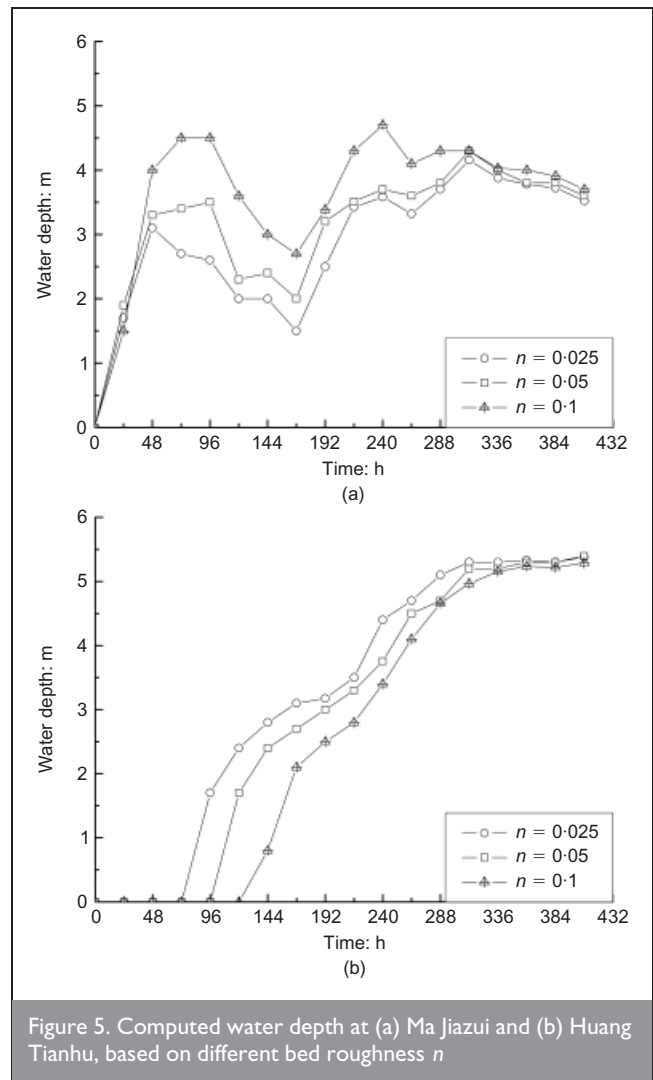


Figure 5. Computed water depth at (a) Ma Jiazui and (b) Huang Tianhu, based on different bed roughness n

(after $t = 300$ h) retained flood water upstream has propagated downstream due to gravity and thus there is almost no difference in the water levels computed with either $n = 0.025$ or 0.1 for both upstream and downstream gauging stations.

It can thus be concluded that, in practice, bed roughness in the flood diversion area could be increased (e.g. by planting trees or building flood barriers) in order to reduce flooding in downstream regions. However, this might be achieved to the detriment of upstream regions.

3.6. Sensitivity test on influence of viscosity term

As mentioned earlier, one of the major improvements of the current PIC model over that of Wang *et al.* (1998) is that the viscosity term has been included to account for the velocity differences between adjacent fluid layers. In order to numerically demonstrate the role of the viscosity term, the model was rerun with and without viscosity; the computed flooded areas and velocity fields 48 h after flood diversion are shown in Figure 6 and 7, respectively.

Figure 6 shows that there is almost no difference in the flooded areas computed with and without the viscosity term. However, from the velocity fields shown in Figure 7, it is very obvious that the computations including the viscosity term (Figure 7(b)) gave a much smoother velocity field. This is because the viscosity term has a dissipation effect that dampens the flow velocity

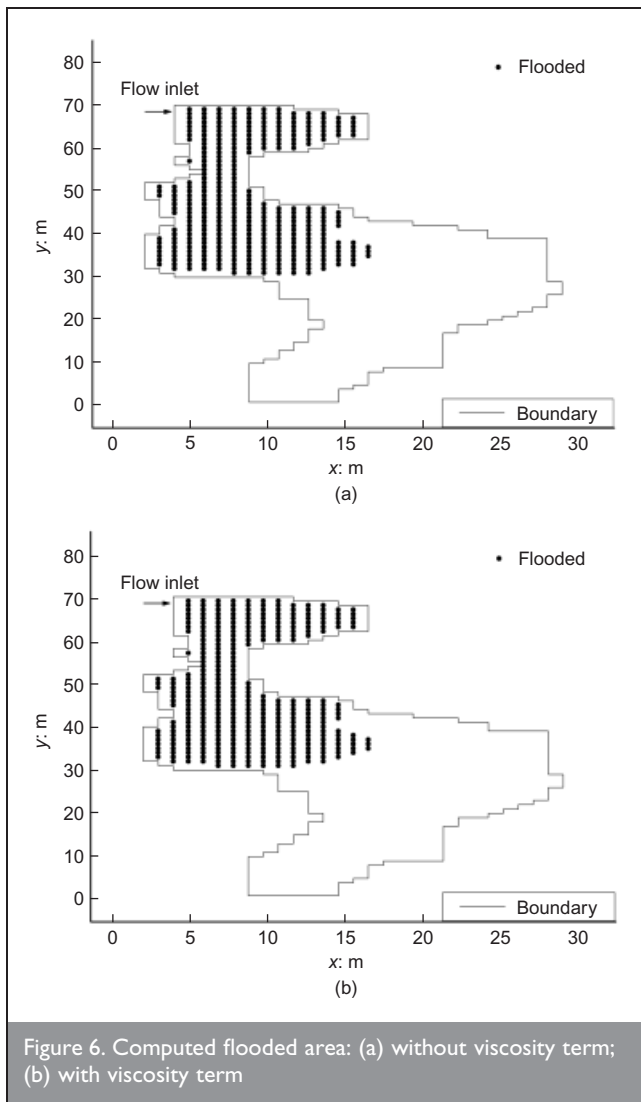


Figure 6. Computed flooded area: (a) without viscosity term; (b) with viscosity term

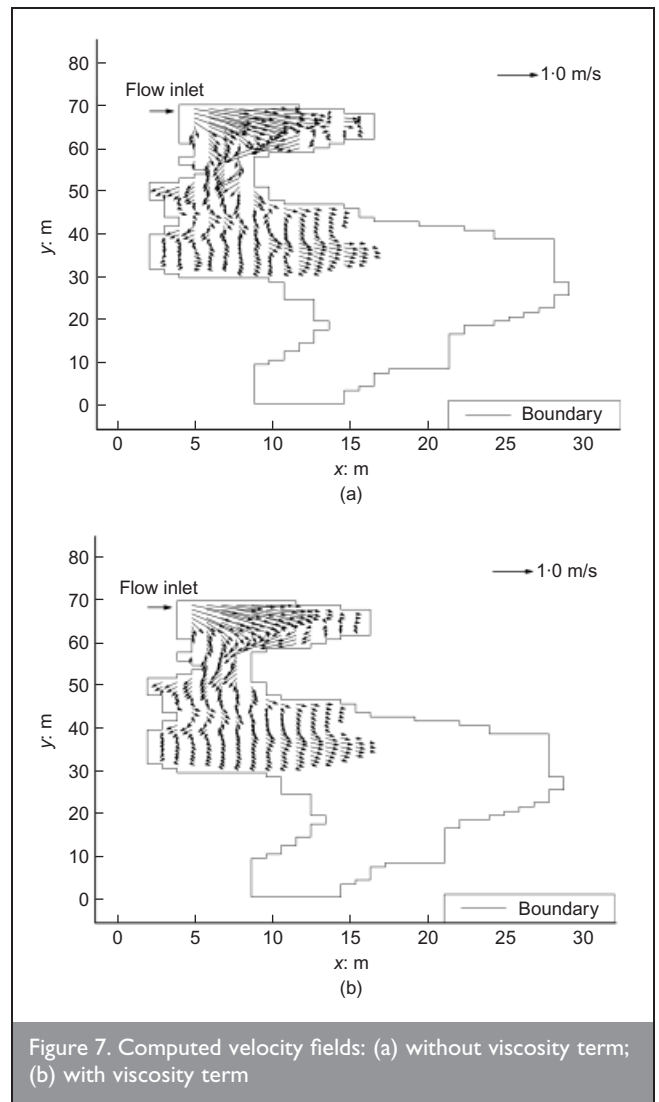


Figure 7. Computed velocity fields: (a) without viscosity term; (b) with viscosity term

gradient and tends to make the flow field more uniform. Thus, in the current model, it could be concluded that the influence of viscosity is less significant on large-scale flow patterns such as flooded area but more noteworthy on refined flow structures such as velocity fields. Therefore, if only water levels or flooded areas are of interest, the model could thus be run without the viscosity term to save computation time in a practical situation. Inclusion of the viscosity term is necessary if more detailed flow features are required, but this will lead to an increase in computation time since the influence of the neighbouring particles is taken into account in the numerical program.

4. CONCLUSIONS

The classic PIC model has been revisited to investigate its numerical stability and accuracy. Numerical tests carried out using different time steps and particle volumes indicate that the stability of the model is constrained by the Courant condition, which is also dependent on the selected particle volume. The Courant coefficient was calculated to be 0.12–0.25 and the spatial accuracy of the model found to be accurate to first-order. The model is simple and straightforward to code and thus provides a useful tool to predict real flooding in a timely manner. By reproducing a documented flood event in 1954 in the Jingjiang River flood diversion area located near the middle and lower reach of the Yangtze River, it was shown that the model can satisfactorily predict flood arrival time and

peak flood levels. Finally, by simulating several flooding processes with different bed roughness values in the flood diversion region, this work has demonstrated that an overall increase in bed roughness can delay flood arrival time and considerably increase flood level in the upstream region. On the other hand, downstream flood levels can decrease significantly due to accumulation of flood water upstream and slow motion of the flood flow. This finding could thus be used to mitigate flood disasters in downstream regions. Computations made with and without inclusion of the viscosity term indicate that the influence of viscosity is more significant on flow velocity fields than on prediction of flooded area.

ACKNOWLEDGEMENTS

This work was supported by a Royal Society research grant (2008/R2 RG080561). The authors are very grateful to the two anonymous reviewers for their invaluable comments on improving the quality of the manuscript.

REFERENCES

- Caleffi V, Valiani A and Zanni A (2003) Finite volume method for simulating extreme flood events in natural channels. In *Journal of Hydraulic Research* 41(2): 167–177.
- Harlow FH (1964) The particle-in-cell computer method for fluid dynamics. In *Journal of Computational Physics* (Alder

- B, Fernbach S and Rotenberg M (eds). Academic Press, New York, pp. 319–343.
- Li W and Huang JG (1993) *Numerical Simulations of the Flood Development in the Jingjiang River Flood-Diversion Area*. Wuhan Hydraulic and Electric University, Wuhan City, China, pp. 1–19 (in Chinese).
- Mingham CG and Causon DM (1998) High-resolution finite-volume method for shallow water flows. *ASCE Journal of Hydraulic Engineering* 124(6): 605–614.
- Nicholas AP and McLelland SJ (2004) Computational fluid dynamics modelling of three-dimensional processes on natural river floodplains. *Journal of Hydraulic Research* 42(2): 131–143.
- Ogami Y (1999) A pure Lagrangian method for unsteady compressible viscous flow. *Computational Fluid Dynamics Journal* 8(3): 383–392.
- Shao SD, Lo EYM and Wang GQ (2002) Simulation of fan formation using a debris mass model. *Journal of Hydraulic Research* 40(4): 425–433.
- Tetzlaff DM and Harbaugh JW (1989) *Simulating Clastic Sedimentation*. Van Nostrand Reinhold, New York, pp. 1–64.
- Wang GQ, Shao SD and Fei XJ (1998) Particle model for simulating flow over large areas. *ASCE Journal of Hydraulic Engineering* 124(5): 554–557.
- Werner MGF and Lambert MF (2007) Comparison of modelling approaches used in practical flood extent modelling. *Journal of Hydraulic Research* 45(2): 202–215.

What do you think?

To discuss this paper, please email up to 500 words to the editor at journals@ice.org.uk. Your contribution will be forwarded to the author(s) for a reply and, if considered appropriate by the editorial panel, will be published as discussion in a future issue of the journal.

Proceedings journals rely entirely on contributions sent in by civil engineering professionals, academics and students. Papers should be 2000–5000 words long (briefing papers should be 1000–2000 words long), with adequate illustrations and references. You can submit your paper online via www.icevirtuallibrary.com/content/journals, where you will also find detailed author guidelines.